Invertis Journal of Renewable Energy, Vol. 5, No. 4, 2015 ; pp. 1-10

Effect of reaction time on structural properties of ZnO:Al films

T.O. BERESTOK[1], A.S. OPANASYUK[1], D.I. KURBATOV[1], H. CHEONG[2]
U.B. TRIVEDI[3*], D. LAKSHMINARAYANA[3], C.J. PANCHAL[4] and PRIYA SURYAVANSHI[4]
[1]Department of Electronics and Computer Technology, Sumy State University, Sumy, Ukraine
[2]Department of Physics, Sogang University, Seoul, South Korea
[3]Department of Electronics, Sardar Patel University, Vallabh Vidyanagar 388120, Gujarat, India
[4]Applied Physics Department, Faculty of Technology and Engineering,
The M.S. University of Baroda, Vadodara-390001
**E-mail: .....*

Abstract

Undoped and Al doped ZnO films are obtained by chemical bath deposition onto glass substrates. Investigations of the effect of reaction time on structural and sub-structural features were carried out using high resolution scanning electron microscopy (SEM) and X-ray diffraction analysis. The effects of deposition time on elemental composition are found. Deposited ZnO and ZnO:Al films have a hexagonal structure with growth texture of [002]. Lattice constants of undoped material weakly depend on the time of synthesis and vary in the range of a = 0.32486-0.32548 nm, c = 0.52064-0.52149 nm. Simultaneously, lattice constants of Al doped ZnO films vary in the wide range: a = 0.32490-0.31997 nm, c = 0.52293-0.52116 nm. The coherent scattering domain size (CSD) of undoped ZnO are in the range of ($L_{(100)}$ = (24.5 - 27.3) nm, $L_{(002)}$ = (26.4 - 28.8) nm, $L_{(101)}$ = (25.0 - 27.1) nm). In the ZnO:Al films the CSD size increased with increasing the duration of their synthesis from 45 to 90 min ($L_{(100)}$ = (19.5 - 52.3) nm, $L_{(002)}$ = (23.2 - 55.0) nm, $L_{(101)}$ = (17.6 - 48.3) nm). Further increase of reaction time up to 120 min led to a significant reduction of the CSD size in all crystallographic directions ($L_{(100)}$ = 38.0 nm, $L_{(002)}$ = 39.0 nm, $L_{(101)}$ = 39.4 nm) which was due to the peculiarities of ZnO:Al growth.

Key words : ZnO; ZnO:Al, chemical bath deposition, structure, sub-structure

1. Introduction

Zinc Oxide is a wide band gap (E_g = 3.3 eV at 300 K) semiconductor with a high electron mobility, large exciton binding energy (60 meV), and excellent thermal and chemical stability [1]. Owing to its unique combination of optical and electro-physical properties, ZnO is of interest for opto-, acousto-electronics, spintronics, sensors, and solar cell device applications [2]. Zinc Oxide is usually *n*-type semiconductor, which is determined by the formation of intrinsic point defects such as oxygen vacancies (V_o) and *Zn* interstisial (Zn_i) in the crystal lattice [3]. One of the effective ways to enhance the conductivity of ZnO is doping by elements of group III of the periodic table. in particular Al, Ga and In [4, 5, 6, 7]. At the same time, aluminum is considered the most promising dopant because it allows obtaining stable low-resistivity material with high transparency in the visible spectrum [8]. In this regard, ZnO:Al is seen as an environmentally friendly alternative to more expensive indium-doped tin oxide (ITO) for use as an effective conductive layer of thin film solar cells [9, 10], microwave absorbing coatings, sterilizer, and antifreeze coatings [11]. In addition, ZnO:Al condensates are widely used as a base material for photocatalysts [12, 13], ethanol sensors [14, 15] and others.

Numerous physical and chemical methods are

used for obtaining undoped and doped thin films and nanostructures of ZnO:Al. They include magnetron sputtering [16], pulsed laser deposition [17], chemical vapor deposition [18], spin-coating [19], spray pyrolysis, [20], electrochemical deposition [21], sol-gel method [22, 23], and chemical bath deposition [24-26]. The advantages of physical methods include the possibility of producing the more advanced structural layers of zinc oxide. Along with this, the main disadvantage of physical methods is the technologically complexity of the process that leads to the high cost of the finished devices. In contrast to the physical methods, chemical processes are characterized by the simplicity and efficiency. Chemical bath deposition (CBD) is one of the most promising among chemical methods because it does not require high temperature and pressure during the process. Moreover, for the deposition of ZnO layers, substrates of different types, shapes and sizes, including flexible, can be used. Also the chemical growth method enables obtaining of condensates with different structural characteristics from nanostructured to continues films [27].

However, commercial use of ZnO in device applications is limited by lack of structural investigation of CBD - ZnO:Al condensates. Additionally, studies of the influence of doping impurity of ZnO on structural and sub-structural properties have attracted special attention.

In the present work we present comparizon of the structural properties of undoped and Al doped ZnO films. Also the results of investigations of influence of physical and chemical conditions of their synthesis on texture quality, lattice constants and coherent scattering domain size (CSD) are presented.

2. Experimental Details

2.1 *Synthesis of ZnO and ZnO:Al Films*

Undoped and Al doped ZnO films were obtained by chemical bath deposition from an aqueous solution by changing the duration and number of immersions in a solution with precursors. As the substrate we used glass which was previously cleaned in acetone, isopropanol and ethanol. Zinc nitrate solution (0.1 M) was used as a precursor for zinc oxide layers. To maintain pH at 10, we added a solution of ammonia. For doping of zinc oxide films, an additional solution of aluminum nitrate and KOH was prepared. Obtained solution was mixed by a magnetic stirrer. The temperature of the chemical reactor was 85°C. The reaction time was varied from 30 to 120 min. It should be noted that after the deposition duration of 60 minutes or more the depletion of the reagents occurred, which led to the termination of films deposition. Therefore the substrates were immersed in a new solution after τ = 60 min. After the deposition, the samples were dried in nitrogen atmosphere and annealed in air at 350°C.

2.2 *Characterization*

Morphology investigations of synthesized samples were performed using a scanning electron microscope (ZEISS Avirguda). Structural studies were made using an X-ray diffractometer (Bruker D8 Advance) with Ni-filtered Kα - radiation of copper anode. The X-ray was focused using the Bragg-Brentano method [28]. The study of obtained XRD patterns was performed using Difwin software. Phase analysis was carried out by comparing the interplanar distances and relative intensities of the investigated samples with the standard according to JCPDS 79-0205 [29]. X-ray signals were normalized to the intensity of the (002) peak of the wurtzite phase of ZnO.

The crystalline quality of the ZnO:Al films was determined by Harris method which was especially convenient for flat samples with axis of the texture tested oriented normal to the surface [28]. The pole density was calculated using the equation :

$$P_i = \frac{\left(I_i / I_{0i}\right)}{\frac{1}{N}\sum_{i=1}^{N}\left(I_i / I_{0i}\right)}$$

where I_i and I_{0i} are the integral intensity of the i-diffraction peak for the film samples and the standards, respectively; and N is the number of lines in the diffraction pattern. Thereafter, the dependences P_i - $(hkl)_i$ and P_i - φ were established, where $(hkl)_i$ is the Miller indexes, φ is the angle between the chosen direction and normal to different crystallographic planes, which correspond to the reflection in the XRD pattern. This angle was determined for the hexagonal cell, using the equations given in Ref. 30. The orientation factor was estimated via equation

$$f = \sqrt{\frac{1}{N}\sum_{i=1}^{N}(P_i - 1)^2}$$

Estimation of the interplanar distances of ZnO hexagonal lattice was carried out from the position of $K_{\alpha 1}$ component of all of the most intense lines present in the X-ray pattern.

Calculation of *a* and *c* lattice parameters of hexagonal cell was performed by formulas

$$a = \frac{\lambda}{2\sin\theta}\sqrt{\frac{4}{3}(h^2 + hk + k^2) + \left(\frac{a}{c}\right)^2 l^2} \qquad (1)$$

$$c = \frac{\lambda}{2\sin\theta}\sqrt{\frac{4}{3}\left(\frac{c}{a}\right)^2 (h^2 + hk + k^2) + l^2} \qquad (2)$$

where λ is the X-rays wavelength.

The ratio *c/a* was considered equal to the value defined in the reference (*c/a* = 1.601) [29]. Further more, in order to obtain precise values of crystallographic constants we used the extrapolation method of Nelson-Riley [31]. The linear approximation of obtained points were carried out using the least squares method by OriginPro software. To clarify the constants *a* and *c* of hexagonal phase we used a graphical method of successive approximations [31]. The process was repeated until the values of *a*, *c*, *c/a* converged (usually 4 iterations).

The average size of CSD, *L* in the films was calculate via Scherrer equation [30]:

$$L = \frac{K\lambda}{\beta\cos\theta},$$

where *K* is the coefficient that depends on the shape of grain (K = 0.94); β is the physical broadening of diffraction lines.

3. Results and Discussion

Features of growth of undoped ZnO films were discussed in [26].

Figure 1 shows SEM images of cross-section and surface morphology of the synthesized Al doped ZnO films. Studies have shown that ZnO:Al layers had good adhesion to the surface of the glass substrates. Films synthesized for τ < 60 min were optically transparent, and with increased thickness, they became white. The final thickness of the zinc oxide films was *d* = 3.2 μm (Fig. 1a).

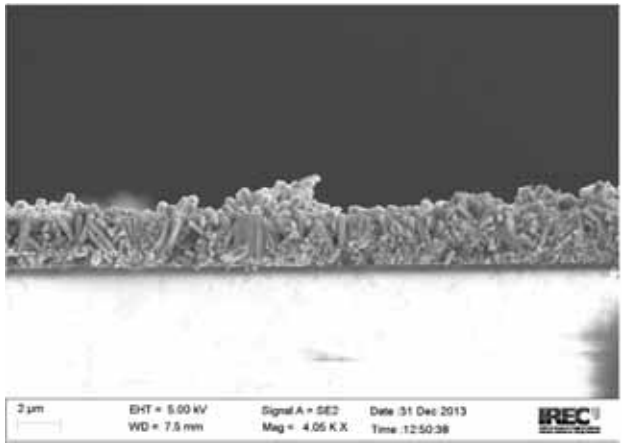

It was established that at the initial stage of the films deposition (τ = 45 min) a densely packed array of grains was formed with mainly hexagonal forms with diameters in the range of 0.5 - 1.0 μm and lengths in the range of ≈ 0.4 μm. The grains were oriented to the axis of [002] and grew at various angles to the substrate (Fig. 1 b). With the increase reaction time (τ = 60 min), the initial layer was covered by hexagonal prismatic nanorods with length of 2 μm and thickness of 0.3-0.5 μm (Fig. 1c). Further increase of the deposition time led to growth of socket with new nanorods. At the same time, the space between nanorods overgrew by filamentous and lamellar crystallites which Fig. 1. SEM images of cross section (τ = 120 min) (a) and morfology of Al doped ZnO films deposited for various reaction time τ, min: 45 (b), 60 (c), 120 (d). Typical EDAX spectra are in the insets indicated changing of growth mechanism. Increasing the deposition time up to 120 min led to increase in the hexagonal rod height (2.5 μm) and thickness (0.5 - 0.8 μm). At the same time nanorods

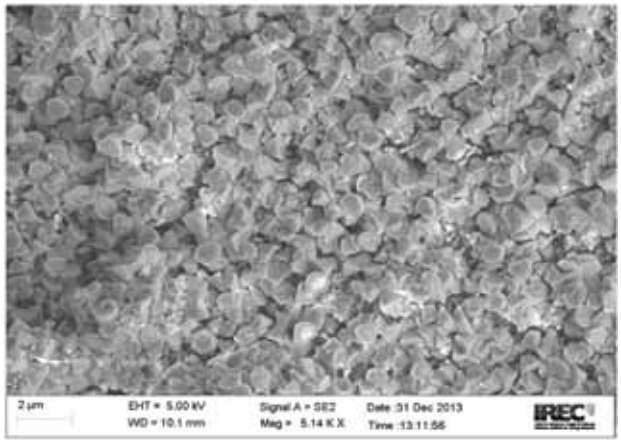

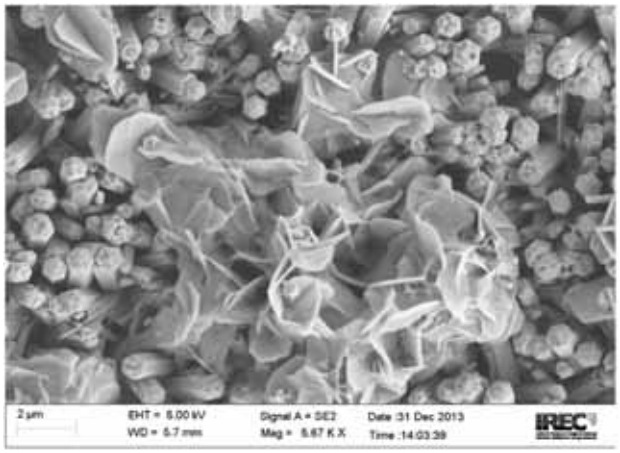

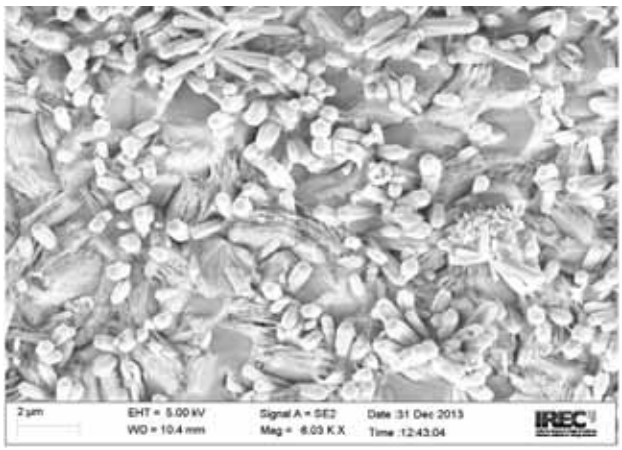

took the form close to the form of poorly sharpened pencil. Additionally, lamellar crystallites overgrew with thickness in the range of 0.1-0.3 µm and lateral dimensions of 2-3 µm.

In order to determine the elemental composition of the doped samples, EDAX analysis was carried out. Typical EDAX spectra of as-grown ZnO:Al layers are shown in Fig. 1 (in the inset). As it can be seen in Figure 2, all EDAX spectra cosist of Zn, O and Al peaks. In the spectra of the films deposited for short time, except the elements belonging to the compound components (Zn, O, Al), we registrated extraneous peaks belonging to elements of the glass substrate (K, Si, Ca). This is due to the fact that these layers were thin and highly porous.

The elemental composition of Al doped ZnO layer determined by EDAX analysis are summarized in Table 1. As it can be seen from the table, increasing the duration of deposition led to reduction of aluminum atomic concentration. This was obviously

Table 1. Elemental Composition of ZnO:Al Films

τ, min	Concentration, at. %			$\frac{C_{Zn+Al}}{C_0}$	$\frac{C_{Zn}}{C_0}$
	Zn	O	Al		
45	17.04	77.33	5.63	0.29	0.22
60	55.32	43.33	1.35	1.31	1.27
90	47.50	48.49	4.01	1.06	0.97
120	33.74	65.35	0.91	0.53	0.52

due to the saturation of the solution and depletion of reactants.

It was found that during the growth of the films, the composition significantly changed. At the initial stage of the synthesis (τ = 45 min), ZnO layers were significantly enriched with oxygen. At the deposition for τ = 60 min, excess of metal was observed. The most stoichiometric films were obtained for reaction time of τ = 60 min. It should be noted that after the synthesis for τ = 60 min, the solution with precursors was refreshed by a new one. Subsequently, solutions depletion resulted to reduction of concentration of metal atoms.

XRD patterns of the synthesized ZnO and ZnO:Al layers are presented in Figure 2. The phase analysis of undoped ZnO films showed [27] that the dominant intensity had reflections from the crystallographic plane (002) of the hexagonal phase of ZnO.

Also in the X-ray patterns, intense lines were registered at the angles of 31.79°, 36.24°, 47.66° of the (100), (101), (102) planes of wurtzite phases of zinc oxide, respectively [29]. As it can be seen from the figure, in the diffraction patterns of undoped films, an extranormous phases were not fixed.

XRD analysis of the ZnO:Al films allowed identifying of peaks with maximal intensity from reflection of (100), (002), (101), (102) crystallographic planes of ZnO hexagonal phase.

In doped samples with small thickness, these lines were shifted in relation to the position characteristic for undoped layers. Moreover in the XRD pattern of thick condensates we have registered the peaks identified as the reflection of the (111) plane of Al cubic phase and (-601) of Al_2O_3 hexagonal phase.

Calculation of the pole density of synthesized

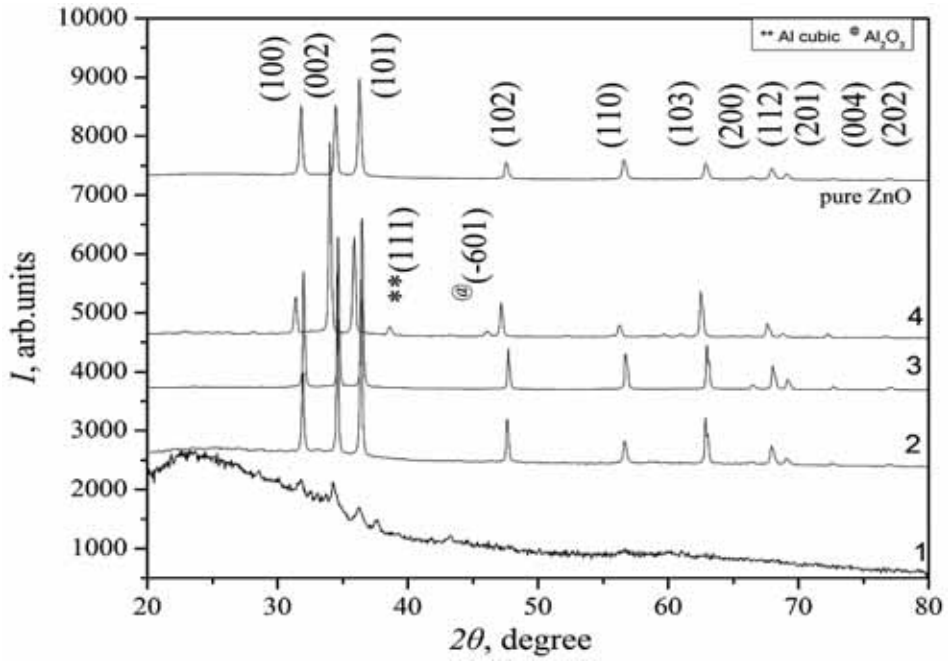

Fig. 2. XRD patterns of undoped (τ = 60 min) and doped ZnO:Al films obtained at various duration of the deposition τ, min: 1 - 45, 2 - 60, 3 - 90, 4 - 120

ZnO and ZnO:Al layers showed (Figure 3) that condensates had weak (f = 0.52 - 1.87 arb. units) axial growth texture of [002]. This growth texture was typical for zinc oxide films obtained by CBD [15]. Dependence of orientation factor f on reaction time of synthesised layers is shown in the inset of Fig. 3.

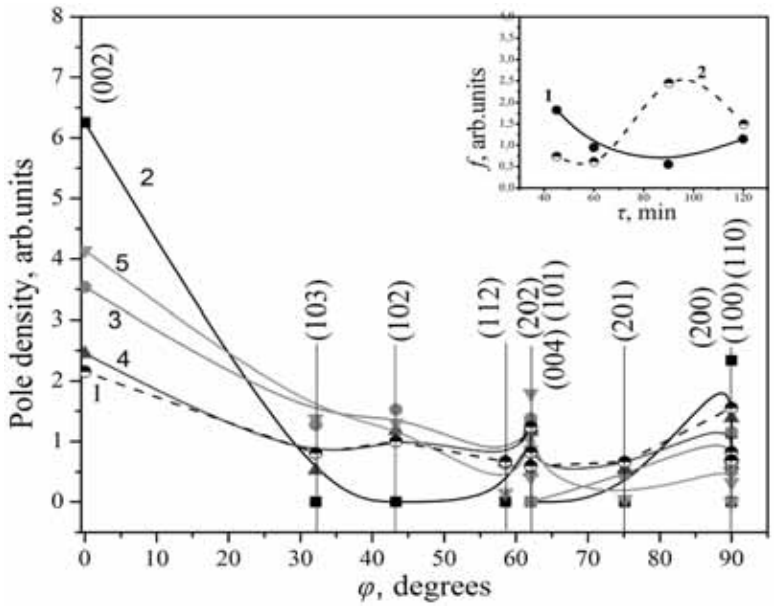

Fig. 3. Dependences of the pole density P_i on the angle φ between the texture axis and the normal to the reflection plane for ZnO films obtained at τ, min: 45 (1), 60 (2), 90 (3), 120 (4). The inset shows dependence of orientation factor f on reaction time fro undoped (1) and doped films (2)

As it can be seen from the figure 3, the quality of ZnO:Al texture decreased after increasing the deposition time. This was due to the peculiarities of film growth and the presence of aluminum atoms in the precursor solution. For undoped films we observed another dependence: increasing the reaction time led to improvement of the crystalline quality. Similar dependence was observed for undoped ZnO films obtained from zinc sulfate and ammonia solutions [26].

We determined the lattice constants of undoped and doped zinc oxide films. Traditionally, the calculation of lattice parameters is carried out with the help of traditional equations using reference value of *c/a* [32]. This results in reduction of the accuracy of calculations. Moreover, it is impossible to determine the *c/a* ratio characteristic for a particular sample. To improve the accuracy of determination of lattice constants *(a, c)* of the material we used the method of successive approximations, including an iterative

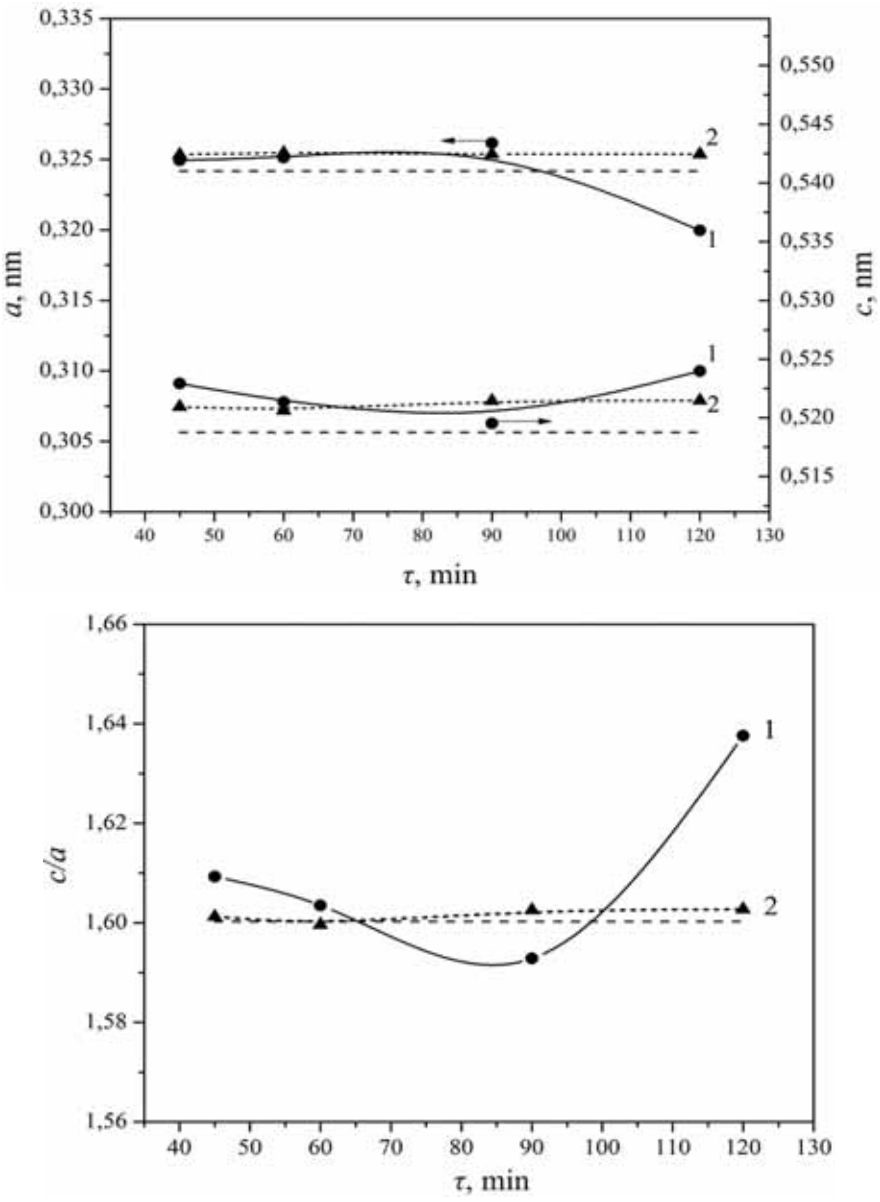

Fig. 4. Dependences of lattice constants *a, c* and their ratio *c/a* (fourth iteration) for doped (1) and undoped (2) ZnO films on the deposition time. The dotted line corresponds to the values of undoped material

procedure described in Ref. 33. As a result of calculations it was found that the values of *a, c* and their ratio *c/a* converged after the fourth iteration, indicating that the procedure of calculation was finished. Therefore these values were used for further analysis.

Fig. 4 showed the dependence of the *a* and *c* lattice constants of ZnO, ZnO:Al films on the duration of the deposition. In the figure the dotted line corresponded to the reference data for undoped ZnO [29].

The values of the lattice parameters of undoped material weakly depended on the reaction time and varried in the range of *a* = 0.32486 - 0.32548 nm, *c* = 0.52064 - 0.52149 nm. Simultaneously, the lattice constants of doped ZnO films varied in a wide range: *a* = 0.32490 -0.31997 nm, *c* = 0.52293 - 0.52116 nm and differed from the values listed in the reference for undoped material (*a* = 0.32417 nm, *c* = 0.51876 nm).

At the same time the value of *a* decreased with increasing duration of condensates deposition, along with this the value of *c* increased.

This effect was obviously caused by the presence of aluminum atoms in the films. The authors of Ref. 19 found that the presence of Al atoms in zinc oxide films led to a decrease of the lattice parameter due to the substitution of Zn atoms by smaller atoms of Al (r_{Zn}^{2+} = 0.074 nm; r_{Al}^{3+} = 0.053 nm) [19].

It was confirmed that increasing the deposition time led to decrease of *c/a* ratio from 1.6093 to 1.5928, with a significant increase of this parameter to 1.6376 at τ = 120 min.

The estimation of the lattice parameters allowed us to carry out the calculation of the unit cell volume of hexagonal lattice and the bond lengths between the atoms of zinc and oxygen in the material (Fig. 5).

The values of the unit cell volume of undoped zinc oxide films were almost independent of the duration of the deposition (*V* = 0.1428-0.1430 nm^3). These values are in good agreement with the reference one (*V* = 0.1435 nm^3).

It was established that the volume of the hexagonal primitive cell of doped films with small thickness (τ = 45-60 min) was *V* = 0.1434 - 0.1430 nm^3. Increasing the deposition time of the layers from τ = 90 min to τ = 120 min resulted in reduction of the unit cell volume from *V* = 0.1436 nm^3 to *V* = 0.1394 nm^3. Simultaneously, bond lengths between the atoms of zinc and oxygen changed from *l* = 0.19802 nm to *l* = 0.19618 nm. These values differed from

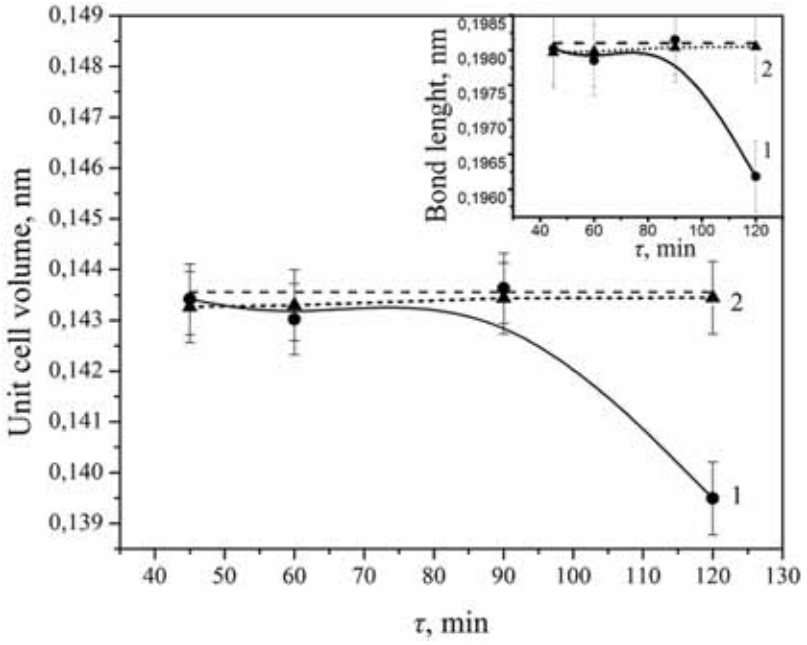

Fig. 5. Unit cell volume V and bond lengths between the atoms of Zn-O (in the inset) of undoped and Al doped ZnO films as a function of reaction time. The dotted line corresponds to the reference data

Table 2. Structural and Sub-structural features of Al Doped ZnO films

τ, min	ZnO:Al									ZnO		
	a, nm	*c, nm*	*c/a*	*a, nm*	*c, nm*	*c/a*	*L, nm*			*L, nm*		
	1st iteration			4th iteration			(100)	(002)	(101)	(100)	(002)	(101)
45	0.3249	0.52293	1.6095	0.32494	0.52293	1.60931	19.5	23.2	17.6	24.5	26.4	25.0
60	0.32513	0.52075	1.6016	0.32513	0.52135	1.60351	45.5	54.0	47,3	25.2	26.1	25.2
90	0.32603	0.52009	1.5952	0.32617	0.51953	1.59282	52.3	55.0	48,3	25.5	28.1	25.7
120	0.32097	0.52116	1.62	0.31997	0.52398	1.63759	38.0	39.1	39,4	27.3	28.8	27.1

the reference ones given to the bulk undoped material (l = 0.19721 nm), which was the result of the presence of Al atoms in the films.

Table 2 shows the results of calculations of the CSD size of the synthesized films. After the deposition for 120 min these values were growing poorly and varried in the range of $L_{(100)}$ = (24.5 - 27.3) nm, $L_{(002)}$ = (26.4 - 28.8) nm, $L_{(101)}$ = (25.0 - 27.1) nm .

As shown in Table 2, the size of CSD of ZnO:Al films increased with increasing the duration of the synthesis from 45 to 90 min ($L_{(100)}$ = (19.5 - 52.3) nm, $L_{(002)}$ = (23.2 - 55.0) nm, $L_{(101)}$ = (17.6 - 48.3) nm. Further increasing the time of deposition up to 120 min caused a significant reduction of CSD size in all crystallographic directions ($L_{(100)}$ = 38.0 nm, $L_{(002)}$ = 39.0 nm, $L_{(101)}$ = 39.4 nm). This behavior was caused by the peculiarities of films growth when at the initial stage of growth there were formed the oriented nanorods in the direction of (002), and with increasing deposition time, the crystallite size increased. Increase of the reaction time up to 120 min led to overgrow the space between nanorods by filamentous and lamellar crystallites with small thickness and resulted in a decrease in the average size of CSD. A similar trend was observed for ZnO:Al films obtained by sol-gel method and spin-coating in Ref. 34. Furthermore, using Scherrer equations, R. Chandramohan et al. obtained similar values of CSD (L = 40.7 - 47.9 nm) for aluminum doped zinc oxide films synthesized from a solutions of zinc sulfate, ammonia and sodium hydroxide [24].

4. Conclusion

A comparison of the structural and substructural characteristics of undoped and Al doped ZnO films synthesized by the method of chemical bath deposition from an aqueous solution of zinc nitrate, ammonia and aluminum nitrate at different reaction time was carried out. It was shown that the growth occurred thought the formation of hexagonal prismatic nanorods followed by overgrowing of filamentous and lamellar crystallites.

It was established that increasing the deposition time of the layers led to a reduction of the concentration of aluminum in films from 5.63 to 1.35 (at τ = 60 min it was the refreshing of the solution), and from 4.01 to 0.91 (τ = 120 min), due to the depletion of chemical reagents during the reaction.

It was shown that the synthesized ZnO and ZnO:Al condensates had a hexagonal structure with growth texture of [002], and the crystalline quality depended on the time of deposition. It was found that lattice constants of undoped material weakly depended on the time of synthesis and varied in the range of a = 0.32486-0.32548 nm, c = 0.52064-0.52149 nm. At the same time, the lattice constants of Al doped ZnO films varied in the wide range: a = 0.32490-0.31997 nm, c = 0.52293-0.52116 nm. The lattice parameter a decreased with increasing the duration of the deposition; and lattice parameter c slightly increased.

The values of CSD of the films obtained at various reaction time were established. It was shown that the CSD ($L_{(100)}$ = (24.5 - 27.3) nm, $L_{(002)}$ = (26.4 - 28.8) nm, $L_{(101)}$ = (25.0 - 27.1) nm) of undoped films weakly increased after increasing of . In the ZnO:Al films the CSD size increased with increasing the duration of their synthesis from 45 to 90 min ($L_{(100)}$ = (19.5 - 52.3 nm, $L_{(002)}$ = (23.2 -55.0) nm, $L_{(101)}$ = (17.6 - 48.3) nm). Further increase of reaction time up to 120 min led to a significant reduction of the CSD size in all crystallographic directions ($L_{(100)}$ = 38.0 nm, $L_{(002)}$ =

39.0 nm, $L_{(101)}$ = 39.4 nm) which was due to the peculiarities of ZnO:Al growth.

5. Acknowledgment

This research was supported by the Ministry of Education and Science of Ukraine (Grant No. 0113U000131, No. 0112U000772 and the individual grant for D.O.) and also thankful to UGC for providing a financial assistance to the department under DRS [file no. 530 / 16 / DRS / 2013(SAP-1)].

References

[1] U. Ozgur, Ya.I. Alivov, C. Liu, A. Teke, M.A. Reshchikov, S. Doğan, V. Avrutin, S.J. Cho, and H. Morkoç, "A comprehensive review of ZnO materials and devices," *J. Appl. Phys.*, **89** (2005) 041301-1-103.

[2] J. Fan, Y. Hao, C. Munuera, M. Garcia-Hernandez, F. Guell, E. M. J. Johansson, G. Boschloo, A. Hagfeldt, A. Cabot," Influence of the Annealing Atmosphere on the Performance of ZnO Nanowire Dye-Sensitized Solar Cells," *J. Phys. Chem.* C, **117**(32) (2013) 16349.

[3] J. D. Fan, A. Shavel, R. Zamani, C. Fabrega, J. Rousset, S. Haller, F. Guell, A. Carrete, T. Andreu, J. Arbiol, J. R. Morante, A. Cabot, " Control of the doping concentration, morphology and optoelectronic properties of vertically aligned chlorine-doped ZnO nanowires," *Acta Mater.*, **59**(17) (2011) 6790.

[4] S. Benramache, B. Benhaoua and H. Bentrah, "Preparation of transparent, conductive ZnO:Co and ZnO:In thin films by ultrasonic spray method," *Journal Of Nanostructure in Chemistry*, **3** (2013) 54.

[5] M.-Ch. Jun, S.-U. Park, J-H. Koh, Jun, "Comparative studies of Al-doped ZnO and Ga-doped ZnO transparent conducting oxide thin films," *Nanoscale Research Letters*, **7** (2012) 639.

[6] E.D. Bourret-Courchesne, S.E. Derenzo, M.J. Weber, "Development of ZnO:Ga as an ultra-fast scintillator," *Nuclear Instruments and Methods in Physics Research* A, **601** (2009) 358.

[7] E. D. Gaspera, M. Bersani, M. Cittadini, M. Guglielmi, D. Pagani, R. Noriega, S. Mehra, A. Salleo, A. Martucci, "Low-Temperature Processed Ga-Doped ZnO Coatings from Colloidal Inks," *J. Am. Chem. Soc.*, **135** (2013) 3439.

[8] D.-J. Kwak, B.-W. Park, Y.-M. Sung, "Bias Voltage Dependence of the Electrical and Optical Properties of ZnO:Al Films Deposited on PET Substrates," *Journal of the Korean Physical Society*, **55**(5) (2009) 1940.

[9] M.Chen, Z.L.Pei, X.Wang, C.Sun, L.S.Wen, "Dependence of structural, electrical and optical properties of ZnO:Al films on substrate temperature," *J. Mater. Res.*, **16** (2001) 2118.

[10] A. Crossay, S. Buecheler, L. Kranz, J. Perrenoud, C.M. Fella, Y.E. Romanyuk, A.N. Tiwari, "Spray-deposited Al-doped ZnO transparent contacts for CdTe solar cells," *Solar Energy Materials & Solar Cells*, **101** (2012) 283.

[11] C.X. Luo, J.K. Liu, Y. Lu, C.S. Du, "Controllable preparation and sterilization activity of zinc aluminum oxide nanoparticles," *Materials Science and Engineering: C*, **32** (2012) 680.

[12] A. Patzko, R. Kun, V. Hornok, I. Dekany, T. Engelhardt, N. Schall, "ZnOAl-layer double hydroxides as photocatalysts for oxidation of phenol in aqueous solution," *Colloids Surf. A: Physicochem. Eng. Aspects*, **265** (2005) 64.

[13] K.C. Hsiao, S.C. Liao, Y.J. Chen, "Synthesis, characterization and photocatalytic property of nanostructured Al-doped ZnO powders prepared by spray pyrolysis," *Materials Science and Engineering: A*, **447** (2007) 71.

[14] W.Y. Zhang, D.K. He, Z.Z. Liu, L.J. Sun, Z.X. Fu, "Preparation of transparent conducting Al-Doped ZnO thin films by single source chemical vapour deposition," *J. Optoelectron. Adv. Mater - Rapid communications*, **4**(11) (2010) 1651.

[15] Z.X. Yang, Y. Huang, G.N. Chen, Z.P. Guo, S.Y. Cheng, S.Z. Huang, "Ethanol gas sensor based on Al-doped ZnO nanomaterial with many gas diffusing channels," *Sensors and Actuators, B: Chemical*, **140** (2009) 549.

[16] B.H. Kong, D.C. Kim, Y.Y. Kim, H. Koun, "Effects of ZnO Template Thickness on the Synthesis of 1-D ZnO Nanostructures," *J. Korean Phys. Soc.*, **49** (2006) S741.

[17] H. Kumarakuru, D. Cherns, "The growth and conductivity of nanostructured ZnO films

grown on Al-doped ZnO precursor layers by pulsed laser deposition", *Ceramics International, in press*.

[18] A. Mohanta, J. G. Simmons Jr., H. O. Everitt, G. Shen, S. Margaret Kim, P. Kung, "Effect of pressure and Al doping on structural and optical properties of ZnO nanowires synthesized by chemical vapor deposition," *J. Lumin.*, **146** (2014) 470.

[19] A. A. Al-Ghamdi, O. A. AlHartomy, M. E. Okr, A.M. Nawar, S. ElGazzar, F. El-Tantawy, F. Yakuphanoglu, "Semiconducting properties of Al doped ZnO thin Films," *Spectrochimica Acta Part A: Molecular and Biomolecular Spectroscopy, in press.*

[20] A. Gahtar, A. Rahal, B. Benhaoua, S. Benramache, "A comparative study on structural and optical properties of ZnO and Al-doped ZnO thin ?lms obtained by ultrasonic spray method using different solvents," *Optik - Int. J. Light Electron Opt., in press.*

[21] J.D. Fan, C. Fabrega, R. Zamani, A. Shavel, F. Guell, A. Carrete, T. Andreu, A.M. Lopez, J.R. Morante, J. Arbiol, A. Cabot, "Solution-growth and optoelectronic properties of ZnO:Cl@ZnS core-shell nanowires with tunable shell thickness," *J. Alloys Compd.*, **555** (2013) 213.

[22] X. Liu, K. Pan, W.Li, D. Hu, Sh. Liu, Y. Wang, "Optical and gas sensing properties of Al-doped ZnO transparent conducting ?lms prepared by sol-gel method under different heat treatments," *Ceramics International*, **40** (2014) 9931.

[23] O. D. Pogrebnjak, T. O. Berestok, Y. Takeda, F .F. Komarov, J. Kassi, Structural properties and elemental composition of Au^+ implanted ZnO films, obtained by sol-gel method, *J. Nano Electron. Phys.*, **6**(2) (2014) 02003.

[24] R. Chandramohan, T.A. Vijayan, S. Arumugam, H.B. Ramalingam, V. Dhanasekaran, K. Sundaram, T. Mahalingam, "Effect of heat treatment on microstructural and optical properties of CBD grown Al-doped ZnO thin films," *Materials Science and Engineering B*, **176** (2011) 152.

[25] S. Kahraman, H.M. Cakmak, S. Cetinkaya, F. Bayansal, H.A. Cetinkara, H.S. Guder, "Characteristics of ZnO thin films doped by various elements," *Journal of Crystal Growth, in press.*

[26] T.O Berestok, D.I. Kurbatov, N.M. Opanasyuk, A.D. Pogrebnjak, O.P. Manzhos, S.M. Danilchenko, "Structural properties of ZnO thin films obtained by chemical bath deposition technique," *Journal of Nano- and Electron Physics*, **5**(1) (2013) 01001.

[27] A. S. Opanasyuk, T. O. Berestok, P. M. Fochuk, A. E. Bolotnikov, R. B. James, "Structural and sub-structural features of chemically deposited Zinc-oxide thin films," *Proc. of SPIE.*, 88232013 (2013) 88230Q-1-6.

[28] B.E. Warren, X-ray Diffraction. Dover Books on Physics, New York, 1990.

[29] Joint Committee on Powder Diffraction Standards (JCPDS card No. JCPDS 79-0205)

[30] Ja. S.Umanskij, Ju. A. Skakov, A. N. Ivanov, L. N. Rastorgujev, Crystallogaphy, X-ray graph and electronmicroscopy, *Metallurgy*, *Moskow*, 632 (1982) (in Russian).

[31] L.S. Palatnik, M.Ya. Fuks, V.M. Kosevych, Mechanism of formation and sub-structure of condensed films, *Nauka, Moskov*, 319 (1972) (in Russian).

[32] A. Drici, G. Djeteli, G. Tchangbedji, H. Derouiche, K. Jondo, K. Napo, J. C. Bernède, S. Ouro-Djobo, M. Gbagba, "Structured ZnO thin films grown by chemical bath deposition for photovoltaic applications," *Phys. stat. sol. A*, **201**(7) (2004) 1528.

[33] D. Kurbatov, H. Khlyap, A. ?panasyuk, "Substrate-temperature effect on the microstructural and optical properties of ZnS films obtained by close-spaced vacuum sublimation," *Phys. Stat. Sol. A.*, **206**(7) (2009) 1549.

[34] Y. Caglar, M. Caglar, S. Ilican, "Microstructural, optical and electrical studies on sol gel derived ZnO and ZnO:Al ?lms," *Current Applied Physics*, **12** (2012) 963.